Applied Radiation and Isotopes 70 (2012) 2170–2175

Contents lists available at SciVerse ScienceDirect

Applied Radiation and Isotopes

journal homepage: www.elsevier.com/locate/apradiso

The effect of impurities on calculated activity in the triple-to-double coincidence ratio liquid scintillation method

Denis E. Bergeron*, Ryan P. Fitzgerald, Brian E. Zimmerman, Jeffrey T. Cessna

Physical Measurements Laboratory, National Institute of Standards and Technology, 100 Bureau Drive, Gaithersburg, MD 20899-8462, USA

ARTICLE INFO

Available online 4 March 2012

Keywords:
Triple-to-double coincidence ratio
TDCR
Liquid scintillation
Impurities
Multilabel

ABSTRACT

In the triple-to-double coincidence ratio (TDCR) method of liquid scintillation counting, unaccounted or improperly accounted impurities can result in lower-than-expected or higher-than-expected recovered activities, depending on the counting efficiency of the nuclide of interest, the counting efficiency of the radionuclidic impurity, and the amount of impurity present. We describe these general dependences using a simple model. The trends predicted by the model are tested experimentally using a series of mixed ^{241}Am/^{3}H and ^{63}Ni/^{3}H sources. An "impurity surface" is derived to facilitate an intuitive grasp of impurity phenomena in TDCR.

Published by Elsevier Ltd.

1. Introduction

We recently reported on ^{241}Pu activity measurements by triple-to-double coincidence ratio liquid scintillation counting (TDCR) (Bergeron and Zimmerman, 2011, Laureano-Perez et al., 2011). Noting previous discord between TDCR and other measurement techniques (NIST, 2008b, Zimmerman, 2008), we focused on photomultiplier statistics, threshold adjustment, minimization of internal reflection, and the beta spectrum shape in the new set of measurements. While accounting appropriately for each of these factors led to incremental improvements in accord between measurement techniques, we also noted that a proper accounting for alpha-emitting impurities led to an increase in the calculated activity. Since we are accustomed to counting schemes in which subtracting counts from a data set leads to a reduction in calculated activity, we found this phenomenon to be somewhat surprising.

In 1992, Simpson and Meyer reported that "small quantities of radioactive impurity that are not accounted for result in a significant reduction in the extracted source activity value" for TDCR measurements on ^{55}Fe. To demonstrate the phenomenon, they performed a set of experiments in which small quantities of ^{137}Cs were added to ^{55}Fe sources; they confirmed that activities calculated without making impurity corrections were significantly lower than when proper impurity corrections were made.

The explanation proffered by Simpson and Meyer for high efficiency impurities causing lower-than-expected calculated activities relies on the relationship between the triple-to-double coincidence ratio, K, and the figure of merit (which is then related to the counting efficiency). In a case with impurities, the triple-to-double coincidence ratio becomes

$$K' = \frac{T+R_2}{D+R_2} \tag{1}$$

where T is the triples rate, D is the doubles rate, and R_2 is the decay rate of an impurity with 100% detection efficiency. For $K<1$, $K'>K$ and so the figure of merit is overestimated and thus a higher-than-expected apparent efficiency is calculated (Simpson and Meyer, 1992). This explanation is satisfying, and intuitively reasonable for small quantities of impurity. However, extending this argument to higher impurity fractions or lower impurity efficiencies proves problematic. Notably, Simpson and co-workers later developed a more sophisticated efficiency tracing-based scheme to measure mixtures of beta-emitting radionuclides (van Wyngaardt and Simpson, 2006, van Wyngaardt et al., 2008).

In the present work, we seek to treat the problem of impurity effects in TDCR more generally. We demonstrate the effects of artificially adding counts (to mimic the effect of adding an alpha-emitting impurity) to a data set. With the aid of several approximations, we develop a simple mathematical model to describe the observed trends, and we discuss its implications. Finally, we describe a set of experiments in which we spike ^{3}H sources with ^{241}Am or ^{63}Ni. The simple model proves remarkably robust, and while it should not be used to make impurity corrections in practice, it makes numerous qualitative predictions that are in accord with experiment. From our equations, we derive three dimensional "impurity surface" plots (calculated activity vs. impurity fraction vs. impurity efficiency) that we think make some of the less intuitive aspects of TDCR impurity effects much more tractable.

* Corresponding author. Tel.: +1 301 975 2282; fax: +1 301 926 7416.
E-mail address: denis.bergeron@nist.gov (D.E. Bergeron).

0969-8043/$ - see front matter Published by Elsevier Ltd.
doi:10.1016/j.apradiso.2012.02.084

2. Methods

Two series of LS sources were prepared and measured via TDCR. Mixed ^{241}Am/^{3}H and mixed ^{63}Ni/^{3}H sources were prepared from standard reference material (SRM) solutions (NIST, 1995, 2007, 2008a) in proportions that maintained a near-constant count rate while varying the "impurity fraction", *f*. *f* is defined as the fraction of "impurity" (^{241}Am or ^{63}Ni) activity relative to ^{3}H activity; sources covering the range $f \approx 0$–0.5 were prepared for both "impurities". The SRMs were dispensed gravimetrically into LS vials containing Ultima Gold AB[1] (PerkinElmer) and the total amount of added acid and water was constant within each series.

The TDCR instrument has been described in detail previously (Bergeron and Zimmerman, 2011, Zimmerman et al., 2004). In the present experiments, data were acquired with a field-programmable gate array (FPGA) system. All of the logical operations for coincidence counting and extending deadtime corrections were handled by LabView code developed in house. The FPGA-based acquisition system was benchmarked against the MAC-3 unit (Bouchard and Cassette, 2000), and will be described in more detail in a future publication; the system as configured for this study recovers the massic activity of a ^{3}H SRM (NIST, 2008a) to within 0.3%.

Efficiency variation was achieved via application of gray filters and variation of the focusing voltage. Four 500 s measurements were performed for each source at each efficiency point. Massic activities were calculated from the raw data (no impurity corrections) and matched blanks using the TDCRB-2 program (Broda et al., 2000), using the ^{3}H spectrum for the efficiency calculations.

3. Results

3.1. Adding counts to data

Fig. 1a shows the effect on calculated activity of artificially adding counts to a ^{241}Pu TDCR data set to numerically mimic the addition of an alpha impurity (or any impurity with very high detection efficiency). As observed by Simpson (Simpson and Meyer, 1992) and later by us (Bergeron and Zimmerman, 2011), small quantities of unaccounted impurities result in a substantial reduction in the calculated activity. The trend towards reduced calculated activity cannot persist indefinitely, and the plot shows a minimum (in this case corresponding to $f \approx 0.1$, where $f = A_i/A_{\text{Pu-241}}$, A_i = the impurity activity, and $A_{\text{Pu-241}}$ = the ^{241}Pu activity) in the ratio of the calculated ^{241}Pu activity to the actual ^{241}Pu activity (R_{calc}/R_1); at sufficiently high impurity fractions, further impurity additions lead to the recovery of higher activities. Panels b and c of Fig. 1 are generated from a simplified TDCR model, the development of which is outlined in the following section.

3.2. Development of a mathematical model

We seek to derive a simple model that captures the most general features of TDCR impurity effects. To make the problem tractable, certain simplifying approximations were made; most notably, we ignored detector asymmetry and adopted a fairly rough form for the counting efficiencies (including approximating the energy spectrum as effectively a single energy). As we show, these approximations are necessary in order to reduce the number of variables to a manageable set and thus reveal general dependences. In section IV, we address the impact of these approximations and discuss how a more rigorous treatment is possible for specific applications.

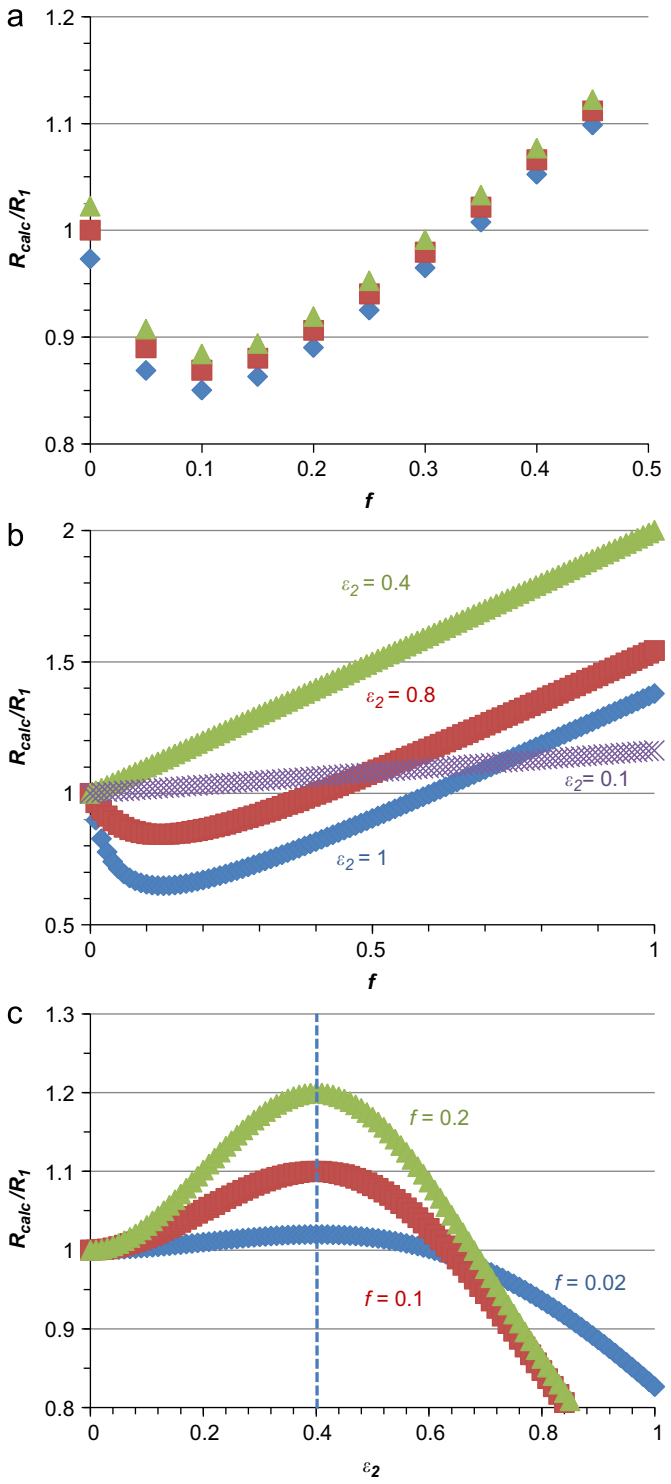

Fig. 1. (a) Calculated massic activity as a fraction of the actual massic activity for a ^{241}Pu source. *f* is varied by adding counts to the raw data to mimic the addition of increasing amounts of an impurity with $\varepsilon = 1$. Then, the massic activities were calculated using the TDCRB-1 program. Diamonds, squares, and triangles correspond to $kB = 0.009$ cm MeV^{-1}, 0.012 cm MeV^{-1}, and 0.015 cm MeV^{-1}, respectively. In (b), a similar trend in the variation of calculated and actual activity with *f* is predicted by our simple model, while (c) highlights the dependence of the calculated activity on the efficiency of the impurity. For both (b) and (c), $\varepsilon_1 = 0.4$. The dotted line in (c) corresponds to $\varepsilon_2 = \varepsilon_1$.

[1] Certain commercial equipment, instruments, or materials are identified in this paper to foster understanding. Such identification does not imply recommendation by the National Institute of Standards and Technology, nor does it imply that the materials or equipment identified are necessarily the best available for the purpose.

Absolute counting efficiencies

$$\varepsilon_{xn} = \frac{\#\text{ of pulses recorded by PMT ``}x\text{''}}{\#\text{ decay events from nuclide ``}n\text{''}} \tag{2}$$

are by nature functions of emission probabilities and energies, scintillation probabilities, quench functions, and PMT quantum efficiencies (Broda et al., 1988, Broda et al., 2007). In the situation described here, we treat ε_{xn} as free parameters, as developed below.

We are interested in the case where a solution containing two nuclides (1 & 2) are counted on a system with three detectors (*A*, *B*, & *C*). The triple-to-double coincidence ratio can be derived (see online supplemental material):

$$K = \frac{R_1\varepsilon_{ABC1} + R_2\varepsilon_{ABC2}}{R_1(\varepsilon_{AB1}+\varepsilon_{BC1}+\varepsilon_{AC1}-2\varepsilon_{ABC1}) + R_2(\varepsilon_{AB2}+\varepsilon_{BC2}+\varepsilon_{AC2}-2\varepsilon_{ABC2})} \tag{3}$$

where R_1 and R_2 are the decay rates for nuclides 1 and 2, respectively, ε_{ABC1} and ε_{ABC2} are the respective triples efficiencies, and ε_{AB1}, ε_{BC1}, ε_{AC1}, ε_{AB2}, ε_{BC2}, and ε_{AC2} are the doubles efficiencies for the indicated nuclide at the indicated PMT pair. Without further assumptions, this complicated equation cannot be simplified, and it is difficult to extract general information on the relationships of the rates and efficiencies. For our current purposes, there is currency in ignoring detection efficiency asymmetry, and assuming that

$$\varepsilon_n = \varepsilon_{An} = \varepsilon_{Bn} = \varepsilon_{Cn} \tag{4}$$

In order to reduce the number of variables, we take the energy spectrum to be monotonic, and approximate the doubles efficiency on any detector pair as ε_n^2, and the triples efficiency, ε_T, as ε_n^3. The logical sum of doubles efficiency is then

$$\varepsilon_{Dn} = 3\varepsilon_n^2 - 2\varepsilon_n^3 \tag{5}$$

and the TDCR is written as

$$K_n = \frac{\varepsilon_n^3}{3\varepsilon_n^2 - 2\varepsilon_n^3} = \frac{\varepsilon_n}{3-2\varepsilon_n} \tag{6}$$

Thus, ε_{Dn} can be written in terms of K:

$$\varepsilon_{Dn} = 3\left(\frac{3K_n}{1+2K_n}\right)^2 - 2\left(\frac{3K_n}{1+2K_n}\right)^3 \tag{7}$$

Now we consider the experimental case in which the nuclide of interest is accompanied by an impurity nuclide. The count rates can be written as

$$N_D = R_1\varepsilon_{D1} + R_2\varepsilon_{D2} \tag{8}$$

$$N_T = R_1\varepsilon_{T1} + R_2\varepsilon_{T2}$$

Written in terms of an impurity fraction, $f = R_2/R_1$, the experimental TDCR is

$$K' = \frac{\varepsilon_{T1} + f\varepsilon_{T2}}{\varepsilon_{D1} + f\varepsilon_{D2}} \tag{9}$$

Eq. (9) is essentially the same expression as Eq. (1), and our Eq. (8) and (9) can be shown to be equivalent to Eqs. (1–7) in (van Wyngaardt and Simpson, 2006). Plotted in Fig. 2a, this expression shows the dependence of K' (shown as a fraction of K, where $K = \varepsilon_{T1}/\varepsilon_{D1}$) on f and ε_2. When ε_2 is less than ε_1, there is a region of f values for which K' is less than K (difficult to see in Fig. 2a, but, for example when $\varepsilon_1 = 0.4$ and $f = 0.2$, K'/K reaches a minimum of ≈ 0.96 at $\varepsilon_2 \approx 0.26$). For higher values of ε_2, K'/K increases monotonically with increasing f. In order to describe the trends in recovered activity, including the nadir in R_{calc}/R_1 in Fig. 1a, it is necessary to solve for the decay rate.

We can use Eqs. (7) and (8) to approximate the decay rate:

$$R = \frac{N_D}{\varepsilon_D} \tag{10}$$

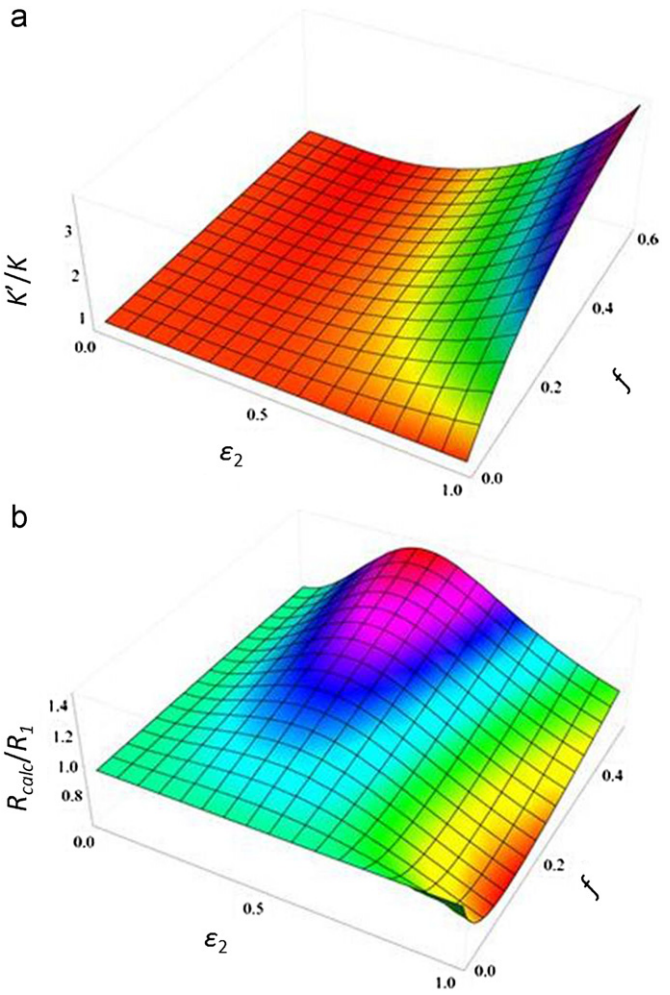

Fig. 2. (a) Three dimensional plot of Eq. (9) showing the monotonic increase of K'/K with increasing f at high ε_2. (b) The ''impurity surface'' derived from Eq. (11). As in Fig. 1, $\varepsilon_1 = 0.4$.

So, by substitution,

$$R_{calc} = \frac{R_1(\varepsilon_{D1} + f\varepsilon_{D2})}{3\left(\frac{3K'}{1+2K'}\right)^2 - 2\left(\frac{3K'}{1+2K'}\right)^3} \tag{11}$$

where R_{calc} is the decay rate expected to be calculated for nuclide 1 if no accounting is made for contributions from nuclide 2, and R_1 is the actual decay rate for nuclide 1. From this equation, it is possible to calculate a relative relationship between the calculated decay rate and the actual decay rate for a set of counting efficiencies and impurity fractions. Fig. 1b, c, and Fig. 2b are derived from Eq. (11), and the general accord with Fig. 1a is excellent.

Fig. 1b shows the behavior of the ratio R_{calc}/R_1 with increasing impurity fraction. The overall behavior can be described in terms of three basic cases:

(a) $\varepsilon_1 = \varepsilon_2$ When the efficiency of the ''impurity'' is equal to the efficiency of the nuclide of interest, the activities simply add, so that when $f = 1$, $R_{calc}/R_1 = 2$. In other words, our model returns the result that adding a quantity of the nuclide of interest to a sample of the nuclide of interest increases the calculated activity by the quantity added. That our model handles this obviously trivial case correctly is reassuring.

(b) $\varepsilon_1 > \varepsilon_2$ When the efficiency of the impurity is lower than the efficiency of the nuclide of interest, an additive trend is

observed, but with slope <1. As with case (a), this result seems intuitive, but it is important that our model returns the expected result.

(c) $\varepsilon_1 < \varepsilon_2$ When the efficiency of the impurity is high relative to the efficiency of the nuclide of interest, R_{calc}/R_1 may become less than 1 at low f. The ratio reaches a minimum and then increases. $R_{calc}/R_1 = 1$ when $f \approx \varepsilon_2 - \varepsilon_1$. This is the case that is not entirely intuitive. It is encouraging that the trends indicated by our simple model agree well with experimental data (*vide infra*).

Fig. 1c shows the behavior of the ratio R_{calc}/R_1 with increasing ε_2. Again it is apparent that when $\varepsilon_1 > \varepsilon_2$—case (b) above—the rates are additive. This behavior persists until $\varepsilon_1 < \varepsilon_2$, where the behavior becomes more complicated. Between the maximum at $\varepsilon_1 = \varepsilon_2$ and the threshold beyond which $R_{calc} < R_1$ lies a region in which the impurity still contributes positively to the calculated rate, but less so than might be anticipated by assuming a linear addition tempered by the relative efficiency. It is again apparent that the $R_{calc} < R_1$ threshold is determined as a function of ε_2 and f; impurities with high detection efficiencies (but relatively low f) lead to lower-than-expected calculated rates. As expected, the maxima and minima in magnitude of the impurity correction are greater for higher impurity fractions, resulting in a cross-over in the curves in Fig. 1c in the $R_{calc} < R_1$ region. For high efficiency impurities, the magnitude of the effect can be quite striking. While these plots should not be interpreted quantitatively, the experimentally observed general dependences between the rates, efficiencies, and impurity fractions are reflected fairly well by our model.

Putting the data from Figs. 1b & c together, the surface in Fig. 2b contains a wealth of information. It can help establish an intuitive feel for the behavior of the ratio R_{calc}/R_1 in the case (c) region. As the case (a) threshold moves along the ε_2 axis, the crossover to and depth of the case (c) region moves in a predictable and understandable manner. As ε_1 becomes very low, the depth of the $R_{calc} < R_1$ portion of the surface increases, while with sufficiently high ε_1, this portion of the plot will disappear altogether. The $1/f$ surface, easy enough to picture, gives the case where the "impurity" and "nuclide of interest" are reversed. While our treatment of this problem arose from handling impurity corrections, it is equally relevant to all cases in which a mixture of radionuclides is present.

3.3. Experiments

The available literature data agree well with the model represented in Eq. 11. However, only a small portion of the surface shown in Fig. 2b is actually sampled by these data. Experiments in which an ^{55}Fe source was spiked with ^{137}Cs (Simpson and Meyer, 1992) provide case (c) data for up to $f \approx 0.04$, and our previous work with α-emitting impurities in a ^{241}Pu solution (Bergeron and Zimmerman, 2011) provide case (c) data up to $f \approx 0.1$. In order to observe the minimum present in the case (c) portion of the surface in Fig. 2b, additional data for higher values of f are required. Our experiments with mixed ^{241}Am/^{3}H and ^{63}Ni/^{3}H sources provide a more complete experimental illustration of impurity effects in TDCR spectrometry.

Fig. 3 shows the fraction R_{calc}/R_1 as a function of f for (a) the mixed ^{241}Am/^{3}H series and (b) the mixed ^{63}Ni/^{3}H series. R_{calc} is the ^{3}H decay rate calculated from the raw TDCR data using the TDCRB-2 code, ignoring the "impurity", while R_1 is the actual ^{3}H decay rate of the standard sample. Fig. 3 also includes lines corresponding to solutions to Eq. 11.

As predicted by Eq. 11 when $\varepsilon_2 = 1$, the experimental data in Fig. 3a show a minimum in R_{calc}/R_1 at approximately $f = 0.1$. We chose ε_1 in order to fit the model to the data. Due to our approximations, the efficiency parameter does not exactly match the experimentally determined counting efficiency. Still, the change in the curve resulting from the addition of a gray filter to the LS source is explained admirably by the model in terms of a reduction in counting efficiency.

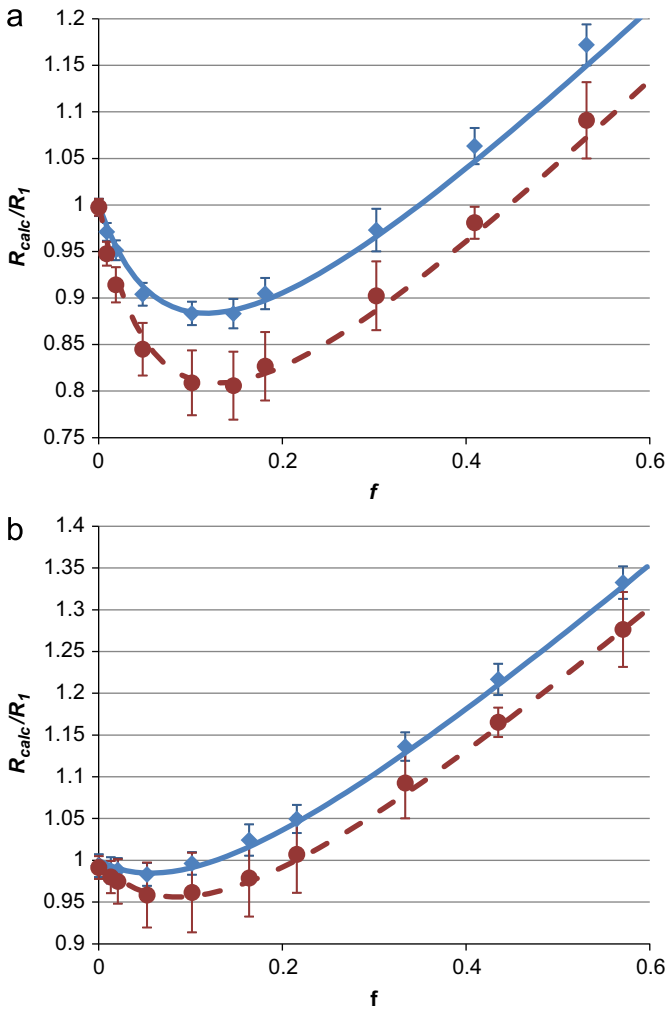

Fig. 3. Calculated massic activity as a fraction of the actual massic activity for a series of ^{3}H sources spiked with (a) ^{241}Am and (b) ^{63}Ni. The diamonds and circles represent data points acquired without and with a gray filter, respectively. In (a), the solid and dashed lines are calculated from Eq. (11) (see online supplemental material for details) using $\varepsilon_1 = 0.525$ and $\varepsilon_1 = 0.480$, respectively. In (b), the solid and dashed lines use $\varepsilon_1/\varepsilon_2 = 0.617$ and $\varepsilon_1/\varepsilon_2 = 0.582$. Uncertainty bars are expanded ($k=2$) combined uncertainties incorporating the uncertainties on the activities of the standards, the measurement repeatability, the single source reproducibility, and the estimated standard uncertainty of mass for each source.

Fig. 3b shows the data from the ^{63}Ni/^{3}H experiment. Because ε_2 is not known *a priori* as in the case of the alpha-emitting impurity, application of the model to the data set is not as simple. The challenge of applying the model to the ^{63}Ni/^{3}H data facilitates a broader enumeration of the shortcomings and successes of our model. The adoption of realistic values for ε_1 and ε_2 reveals that the model can be fit to the experimental data, and one can easily refine the efficiencies to achieve an excellent fit. By fitting the data in this manner, it becomes readily apparent that a continuum of values for ε_1 and ε_2 can be reasonably selected, as long as the ratio of $\varepsilon_1/\varepsilon_2$ is held constant for a given experimental efficiency point. For example, in Fig. 3b, any combination of ε_1 and ε_2 for which $\varepsilon_1/\varepsilon_2 = 0.617$ will yield a curve that fits the

experimental data taken with no gray filter; with filter #2, $\varepsilon_1/\varepsilon_2$ must be set to 0.582.

The ratio $\varepsilon_1/\varepsilon_2$ can be estimated experimentally by reference to the data taken on pure ^{63}Ni and ^{3}H sources by extracting the single-PMT efficiencies from the observed double or triple efficiencies. We found that the experimental ratios were $\approx$20% lower than the ratios required for a good fit in the model, resulting in recovered values for R_{calc}/R_1 that were up to $\approx$20% lower. Similarly, the tritium efficiency, ε_1, derived from the experimental data was $\approx$14% lower than the value required for a good fit in the model, so that values for R_{calc}/R_1 recovered from the ^{241}Am/^{3}H data set were up to $\approx$14% lower.

4. Discussion

The model we have presented here accurately describes the trends in the data, but the quantitative accuracy depends on the free efficiency parameter. Fig. 1a and b show remarkably similar trends, but do not reproduce the same numbers. Similarly, our experiments show that the model can be fit to data using somewhat realistic values for the efficiencies, but poor fits are achieved using the actual efficiencies derived from standards. Due to numerous approximations and assumptions, we do not expect the model to make accurate quantitative predictions. We have already mentioned the assumption of perfect symmetry amongst the three PMT detectors; accounting for detector asymmetry is known to significantly improve the tracking of activity vs. K (Broda, 2003). In addition, in this preliminary study, we have treated all data taken with the same gray filter as having a single efficiency. Efficiency variation is a crucial part of experimental activity determination by TDCR (Broda, 2003, Cassette et al., 2000). In samples with more than one nuclide, accounting for the effects of efficiency variation will be slightly more complicated; the two nuclides will exhibit different relative responses to chemical quenching, gray filter application, and/or PMT voltage variation and so the ratio $\varepsilon_1/\varepsilon_2$ will be different for every efficiency point. A more accurate treatment than the preliminary one presented here would account for the efficiency variation achieved by varying the focusing voltage of the PMTs and for the variation in efficiency due to inexact cocktail matching within the series.

In addition, a more rigorous approach would include the details of the efficiency functions (including emission energies and abundances, scintillation efficiencies, quench functions, and PMT quantum efficiencies). Indeed, substitution of Poissonian expressions for single-valued efficiencies results in subtle changes to the surface depicted in Fig. 2b, but the main features of the surface are preserved. Further difficulties arise when the energy spectra of the emitters are considered. The doubles counting efficiency (triples counting efficiency) is actually derived from the sum over all of the squared (cubed) efficiency terms for the energy spectrum of the emitter. To reduce the number of variables, we approximated the doubles efficiency on any detector pair as ε_n^2, and the triples efficiency as ε_n^3. For non-monoenergetic emitters, the model we have presented approximates the sum of squares (or cubes) as the square (or cube) of the sum. This is obviously incorrect, but the approximation is critical to solving for the efficiency parameter in terms of K, thus allowing us to extend our model to a general form that reveals something of the nature of impurity effects in TDCR counting. Our approximations will prove least detrimental for nuclides that can be approximated as monoenergetic emitters and for nuclides with very high counting efficiency. Despite the numerous assumptions and approximations, our simple model qualitatively describes real phenomena in TDCR counting. We suspect that an "impurity surface" derived from a more rigorous treatment (necessarily case-specific) will share identifiable features with the basic surface in Fig. 2b.

Making appropriate impurity corrections means subtracting from the raw data all counts contributed by impurities. In the case of α-emitting impurities, corrections are trivial so long as an accurate determination (whether by energy thresholding on the TDCR spectrometer or by some other appropriate method) of the impurity activity is performed. For all other impurities, the accurate determination of the impurity activity must be accompanied by some knowledge (usually calculated from a model) of the counting efficiency. If appropriate impurity corrections are made prior to any data analysis, then even the qualitative trends discussed herein are unimportant. The main utility of this work, then, is to foster an understanding of the qualitative impact that improper corrections can be expected to have on recovered activities in TDCR. Because some of these effects are somewhat counterintuitive, we find the three dimensional impurity surface to be a tremendously useful tool. In our laboratory, it is not uncommon to perform preliminary analyses of data to monitor the progress of an experiment. In many cases, these preliminary analyses are performed without the benefit of impurity measurements. Equipped with a better understanding of the nature of impurity effects in TDCR, we anticipate fewer future instances of shock at unexpected and/or counterintuitive results.

5. Conclusions

Unaccounted or improperly accounted impurities can affect recovered activities in TDCR in ways that are not immediately intuitive. As Simpson first reported (Simpson and Meyer, 1992), in the measurement of nuclides with low counting efficiency, small amounts of unaccounted high counting efficiency impurities lead to lower-than-expected recovered activities. Intuitively, we expect that there must be a threshold of impurity fraction (f) beyond which further impurity additions contribute positively to the recovered activity, but an explanation based solely upon the relationship between K' and the counting efficiency implies no inflection in the K' vs. f curve. We presented an extended set of general equations to approximate the ratio R_{calc}/R_1, which is a measure of the degree to which the recovered activity is lower (or higher) than expected.

The ratio R_{calc}/R_1 varies with f in a predictable way, depending on the ratio $\varepsilon_1/\varepsilon_2$. We discussed the behavior when (a) $\varepsilon_1/\varepsilon_2=1$, (b) $\varepsilon_1/\varepsilon_2>1$, and (c) $\varepsilon_1/\varepsilon_2<1$. The phenomenon described by Simpson (1992) corresponds to case (c). Our equation accurately predicts a nadir in the R_{calc}/R_1 vs. f curve when $\varepsilon_1/\varepsilon_2 \ll 1$.

Improperly accounted impurities can have large effects on recovered activities. Depending on the region of the "impurity surface" that applies to the measurements, subtracting too many or too few counts can lead to higher-than-expected or lower-than-expected recovered activities.

Experiments with mixed ^{241}Am/^{3}H and ^{63}Ni/^{3}H sources probed R_{calc}/R_1 over an extensive range of f and two values for ε_2. The general trends in the data consistently matched the predictions derived from Eq. (11). The three dimensional "impurity surfaces" derived from Eq. (11) promote an intuitive feel for the effects that unaccounted and improperly accounted impurities have on TDCR measurements.

References

Bergeron, D.E., Zimmerman, B.E., 2011. TDCR Measurements on Pu-241 at NIST. In: Cassette, P. (Ed.), LSC 2010, Advances in Liquid Scintillation Spectrometry, Radiocarbon, Paris, France, pp. 171–179.

Bouchard, J., Cassette, P., 2000. MAC3: an electronic module for the processing of pulses delivered by a three photomultiplier liquid scintillation counting system. Appl. Radiat. Isot. 52, 669–672.

Broda, R., 2003. A review of the triple-to-double coincidence ratio (TDCR) method for standardizing radionuclides. Appl. Radiat. Isot. 58, 585–594.

Broda, R., Cassette, P., Kossert, K., 2007. Radionuclide metrology using liquid scintillation counting. Metrologia 44, S36–S52.

Broda, R., Pochwalski, K., Radoszewski, T., 1988. Calculation of liquid-scintillation detector efficiency. Appl. Radiat. Isot. 39, 159–164.

Broda, R., Cassette, P., Maletka, K., Pochwalski, K., 2000. A simple computing program for application of the TDCR method to standardization of pure-beta emitters. Appl. Radiat. Isot. 52, 673–678.

Cassette, P., Broda, R., Hainos, D., Terlikowska, T., 2000. Analysis of detection-efficiency variation techniques for the implementation of the TDCR method in liquid scintillation counting. Appl. Radiat. Isot. 52, 643–648.

Laureano-Perez, L., Collé, R., Fitzgerald, R.P., 2011. Standardization of Pu-241: issues and problems. In: Cassette, P. (Ed.), LSC 2010, Advances in Liquid Scintillation Spectrometry, Radiocarbon, Paris, France, pp. 321–329.

NIST, 1995. Standard Reference Material 4226C: Nickel-63 Radioactivity Standard.

NIST, 2007. Standard Reference Material 4322C: Americium-241 Radioactivity Standard.

NIST, 2008a. Standard Reference Material 4927F: Hydrogen-3 Radioactivity Standard.

NIST, 2008b. Standard Reference Material 4340B: Plutonium-241 Radioactivity Standard.

Simpson, B.R.S., Meyer, B.R., 1992. Further investigations of the TDCR efficiency calculation technique for the direct determination of activity. Nucl. Instrum. Methods Phys. Res. A 312, 90–94.

van Wyngaardt, W.M., Simpson, B.R.S., 2006. A simple counting technique for measuring mixtures of two pure beta-emitting radionuclides. Nucl. Instrum. Methods Phys. Res. A 564, 339–346.

van Wyngaardt, W.M., Simpson, B.R.S., Jackson, G.E., 2008. Further investigations of a simple counting technique for measuring mixtures of two pure beta-emitting radionuclides. Appl. Radiat. Isot. 66, 1012–1020.

Zimmerman B.E., 2008. The use of *Mathematica* in analyzing data from the triple-to-double coincidence ratio method (TDCR) for the standardization of radionuclides. LSC 2008, Advances in Liquid Scintillation Spectrometry. Davos, Switzerland.

Zimmerman, B.E., Collé, R., Cessna, J.T., 2004. Construction and implementation of the NIST triple-to-double coincidence ratio (TDCR) spectrometer. Appl. Radiat. Isot. 60, 433–438.